Supplementary Information (SI) for Sustainable Energy & Fuels.

Supporting Information

Doping fluoride into ternary FeCoNi hydroxide electrocatalysts to boost oxygen evolution reaction

Wen-Ju Lu, Tzung-Wen Chiou*

Department of Chemistry, Tunghai university, Taichung, 407224 Taiwan

Email: twchiou@thu.edu.tw

Experimental section

Chemicals. $Fe(NO_3)_3 \cdot 9H_2O$ (99.95 %), $Co(NO_3)_2 \cdot 6H_2O$ and $Ni(NO_3)_2 \cdot 6H_2O$ were purchased from Sigma-Aldrich. Potassium fluoride (99 %) was bought from Acros Organics. KOH (99 %) was purchased from Duksan. All chemicals were used directly without further purification. Ultrapure water (18.2 MΩ) used in the experiments was supplied by a Millipore System (Direct-Q® 3).

Electrode Preparation. The electrodeposition was carried out with a standard three-electrode electrochemical cell containing nickel foam (NF) (surface area: 0.08 cm^2), a graphite rod (L 100 mm, diam. 3 mm) and a saturated calomel electrode (SCE) as the working, auxiliary and reference electrodes, respectively. In order to some physical characterizations, electrodepositions on graphite plate electrodes as the working electrode were performed. The electrolyte solution of $FeCoNiF(OH)_x$ was prepared; $Fe(NO_3)_3 \cdot 9H_2O$ (0.404 g, 1.0 mmol), $Co(NO_3)_2 \cdot 6H_2O$ (0.582 g, 2.0 mmol), $Ni(NO_3)_2 \cdot 6H_2O$ (0.291 g, 1.0 mmol) and KF (0.116 g, 2.0 mmol) were dissolved in 20 mL DI water. The electrolyte solution of $FeCoNi(OH)_x$ was prepared; $Fe(NO_3)_3 \cdot 9H_2O$ (0.404 g, 1.0 mmol), $Co(NO_3)_2 \cdot 6H_2O$ (0.582 g, 2.0 mmol) and $Ni(NO_3)_2 \cdot 6H_2O$ (0.291 g, 1.0 mmol) were dissolved in 20 mL DI water. $FeCoNiF(OH)_x$ and $FeCoNi(OH)_x$ were prepared though controlled potential electrolysis at -1.10 V (vs SCE) for 1000 s at ambient temperature. After deposition, the alloys by careful rinse with water were directly used for electrochemistry tests.

Physical characterization. Powder X-ray diffraction (pXRD) data were obtained using a Bruker D8 X-ray Powder Diffractometer with a Cu K-α radiation source in the range 2θ = 5-100°. Scanning electron microscopy (SEM) images were obtained with a JSM-

6510 microscope (JEOL) equipped. The morphologies of samples were characterized on a transmission electron microscope (TEM, JEOL JEM-1400, Japan) by dropping sample solutions on Cu grids. HRTEM images were obtained with a JEM-2010 microscope (JEOL) equipped. X-ray photoelectron spectroscopy (XPS) spectra were collected on a ULVAC-PHI XPS spectrometer equipped with a monochromatized 1486.6 eV Al Kα X-ray line source directed 45° with respect to the sample surface. The spectra were registered at a base pressure of $<5\times10^{-10}$ torr. Low-resolution survey scans were acquired with a 100 μm spot size between the binding energies of 1-1100 eV. High-resolution scans with a resolution of 0.2 eV were collected between 700.6-744.6 (for Fe), 770-814.8 (for Co), 840.2-883.8 (for Ni), 678.2-698 (for F) and 523-543 (for O) eV.

Electrochemical measurements. All electrochemical experiments were performed with a CH Instrument 621b potentiostat. Fundamental electrochemical testing was carried out, consisting of samples as the working electrode, a graphite rod (L 100 mm, diam. 3 mm) auxiliary electrode and a saturated calomel electrode (SCE) reference electrode. All potentials reported in this paper were converted from vs SCE to vs reversible hydrogen electrode (RHE). RHE = SCE + 0.241 + 0.059×pH. In all experiments, the iR compensation was performed by CHI model 621b software. The linear sweep voltammetry (LSV) curves were obtained in 1.0 M KOH at a scan rate of 2 mV/s. Tafel slopes were calculated using the Polarization curves by plotting overpotential against log(current density). Controlled potential electrolysis (CPE) experiments were conducted in 1.0 M KOH stirred constantly. The auxiliary electrode in CPE cell was separated from the solution of the working electrode by a medium-porosity sintered-glass frit. The electrochemically active surface area (ECSA) was evaluated in terms of double-layer capacitance. Cyclic voltammogram (CV) scans were

conducted in static solution by sweeping the potential from the more positive to negative potential and back at 5 different scan rates: 20, 40, 60, 80 and 100 mV s^{-1}. The capacitance was determined from the tenth cyclic voltammetry curve of each scan rate. The electrochemical double-layer capacitance, C_{DL}, as given by $i_c = vC_{DL}$ (i_c: current density from CV, v: scan rate). The specific capacitance for a flat surface is generally found to be in the range of 20-60 mF cm^{-2}. We used a value of 40 $mFcm^{-2}$ in the following calculations of the electrochemical active surface area. The electrochemical impedance spectroscopy (EIS) measurements were carried out in a frequency range of 0.01 Hz to 100 kHz with an amplitude of 5 mV at an overpotential of 243 mV. The curve fitting was performed by Zview2 software.

ICP-MS experiment. In order to ICP-MS experiment, electrodepositions on copper foam as the working electrode were performed. ICP-MS was performed on a Thermo Scientific™ Element 2™ (Germany). Dry sample was dissolved in concentrated HNO_3.

Determinations of Faradaic Efficiency and TOF. Quantification of the produced O_2 gas was performed by gas chromatography (Chromatec-Crystal 9000) equipped with a micropacked column (ShinCarbon ST #19808, Restek) and thermal conductivity detector (TCD). Helium was used as the carrier gas. Calibration curves were built by the injection of the known amounts of pure O_2. Faradaic efficiency (%) = $(V_{O2}/24.5)\times100\%/(Q_{CPE}/4F)$ where V_{O2} is the volume (L) of O_2 gas by GC detection, Q_{CPE} is the charge (C) during CPE and F is the Faraday constant.

The TOF (s^{-1}) can be calculated with the following equation: TOF = $Q_{CPE}/4Fnt$ where Q_{CPE} is the charge (C) during CPE, F is the Faraday constant, n is the number of Fe

atom (mol) and t is time (s) during CPE.

a. b.

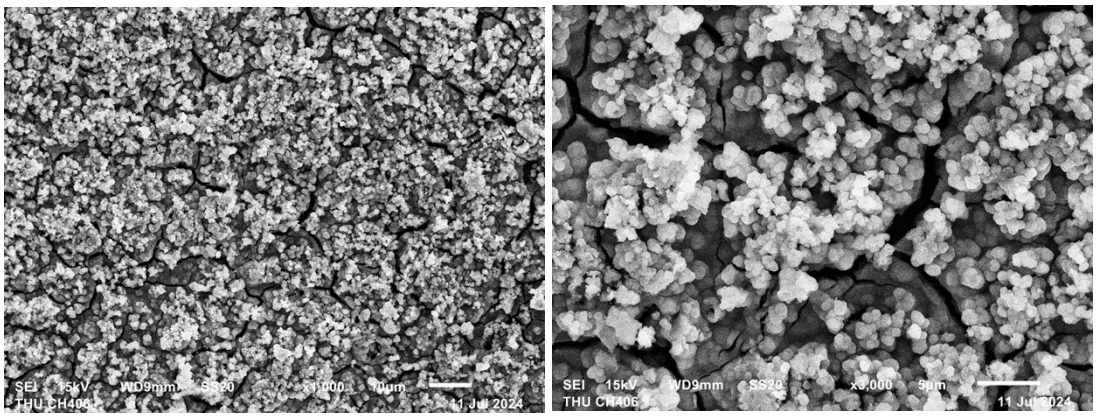

Figure S1. SEM images of $FeCoNi(OH)_x$ (scale bar: 10 μm for a, 5 μm for b).

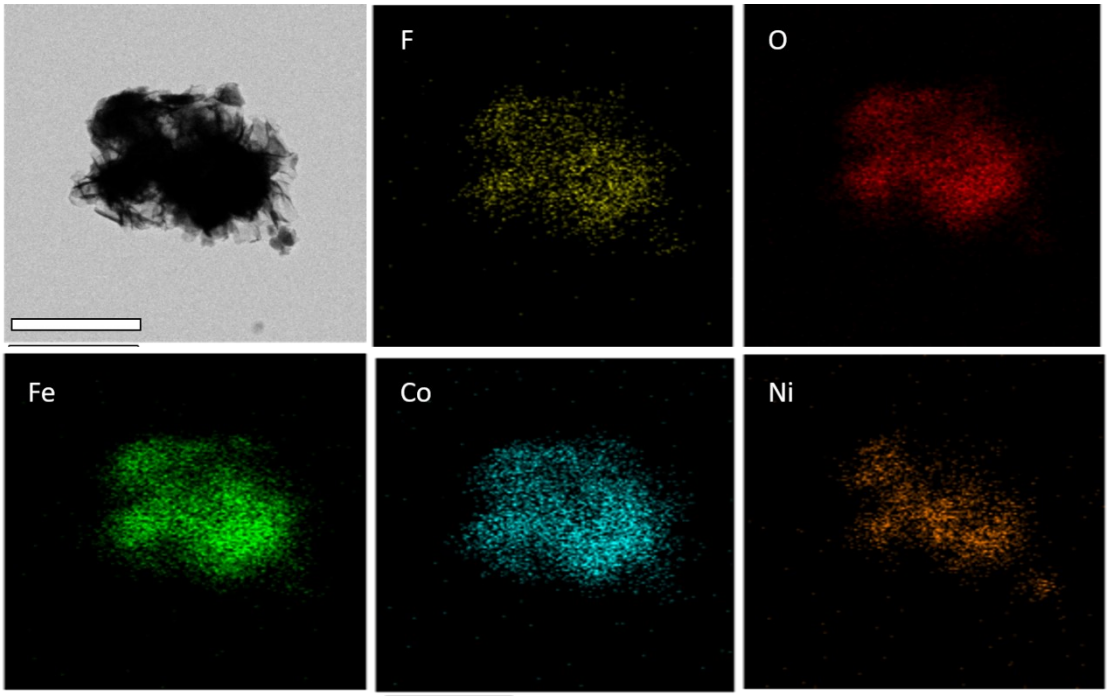

Figure S2. Elemental mapping images of $FeCoNiF(OH)_x$ (scale bar: 1 μm).

a. b.

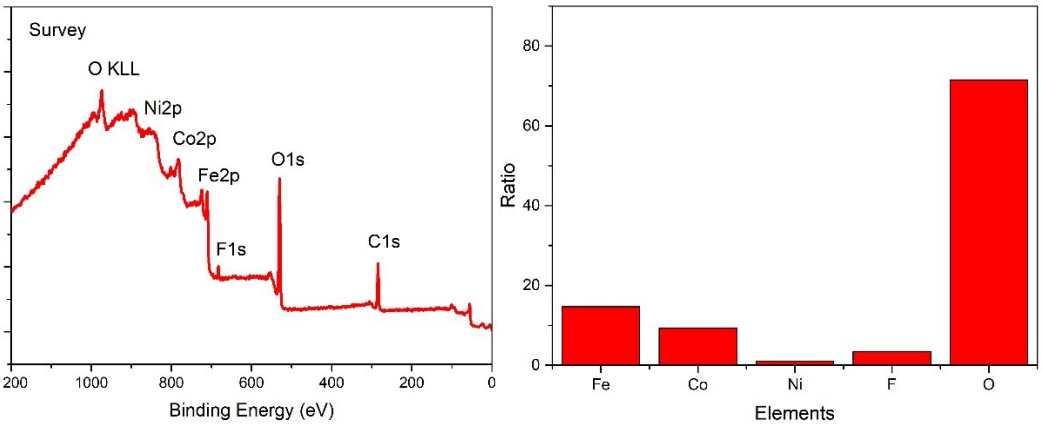

Figure S3. (a) XPS survey spectrum of $FeCoNiF(OH)_x$ and (b) elemental compositions.

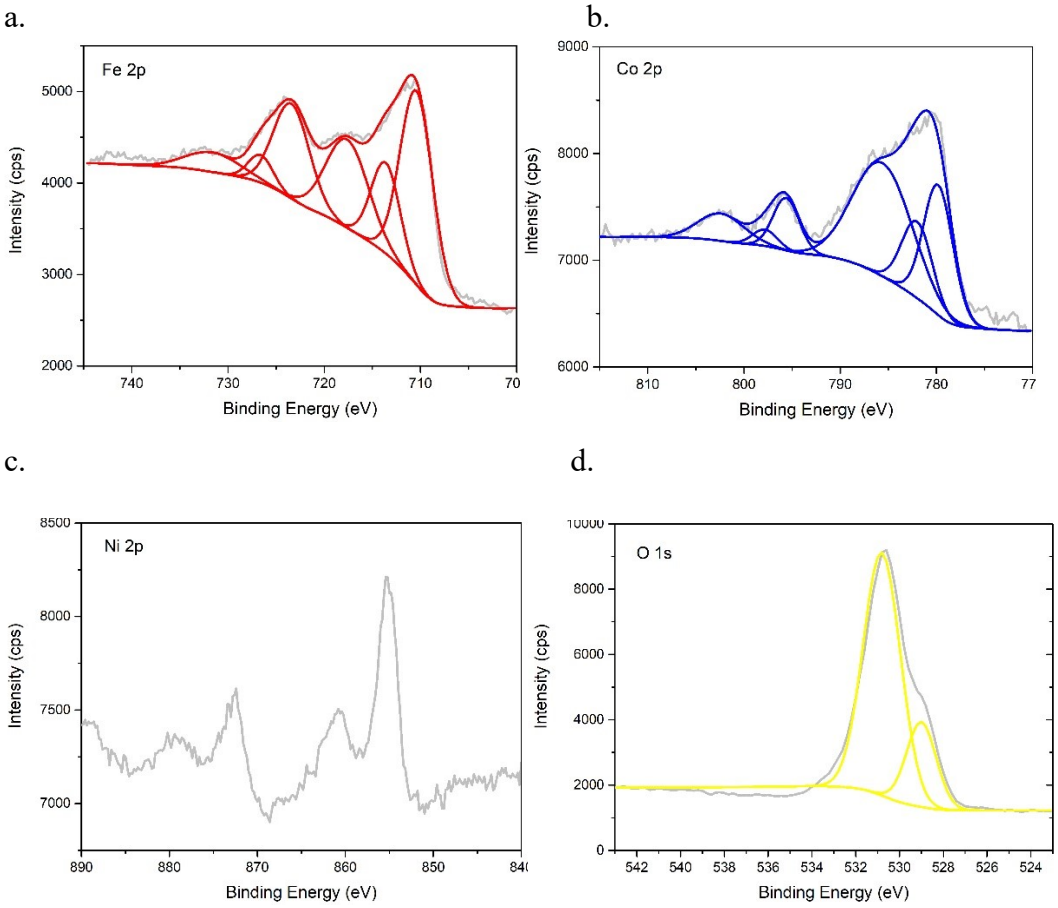

Figure S4. XPS spectra of $FeCoNi(OH)_x$: (a) Fe 2p, (b) Co 2p, (c) Ni 2p and (d) O 1s.

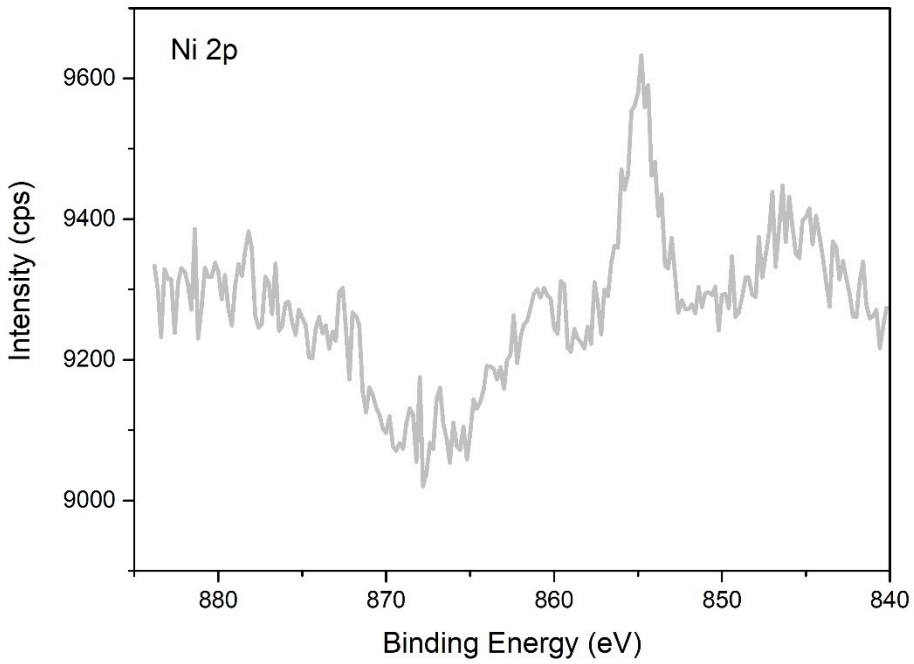

Figure S5. Ni 2p XPS spectra of $FeCoNiF(OH)_x$.

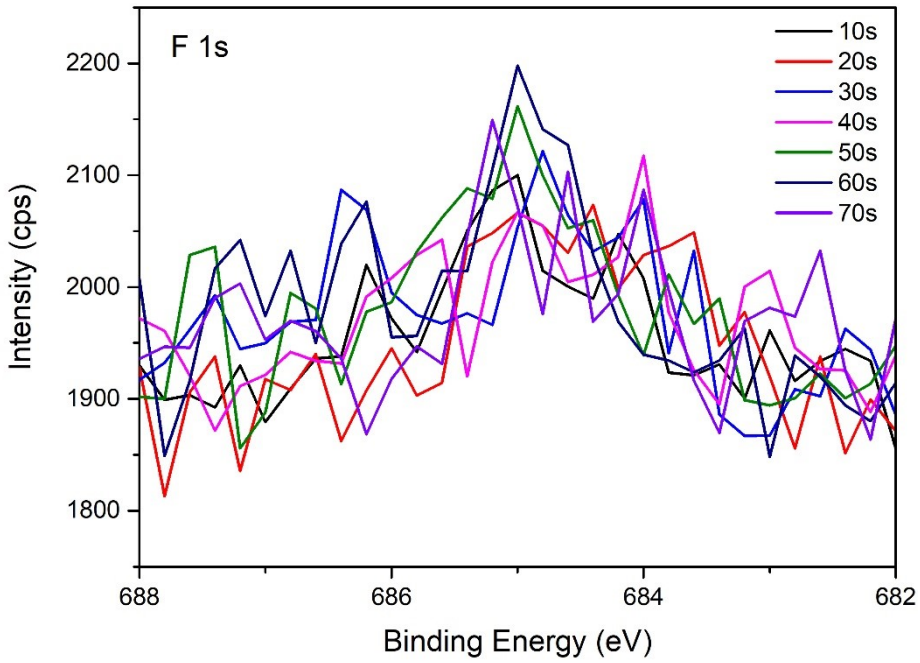

Figure S6. XPS depth profile of $FeCoNiF(OH)_x$. Subsequent scans were taken after additional 10s Ar sputters.

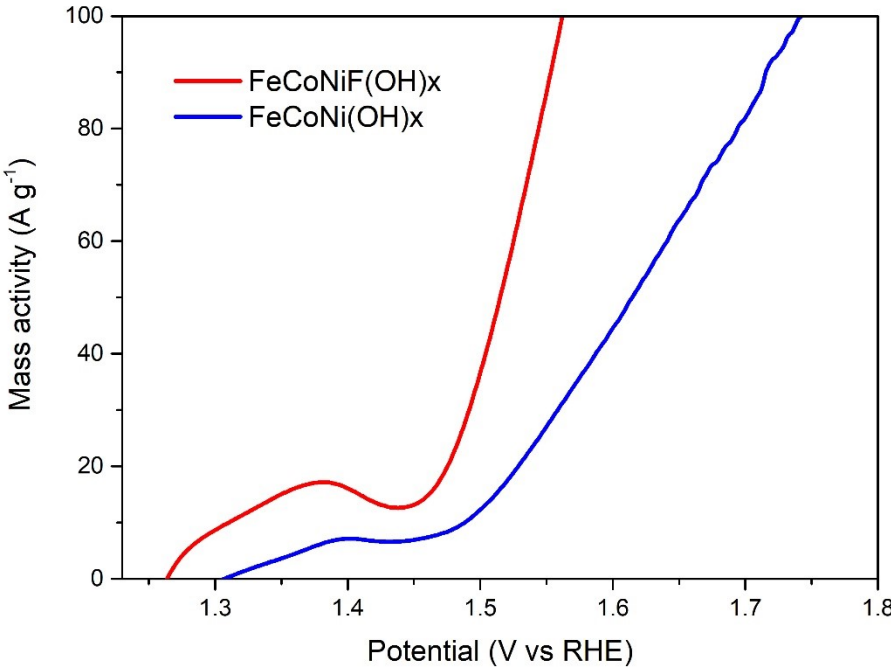

Figure S7. Mass activity of $FeCoNiF(OH)_x$ and $FeCoNi(OH)_x$.

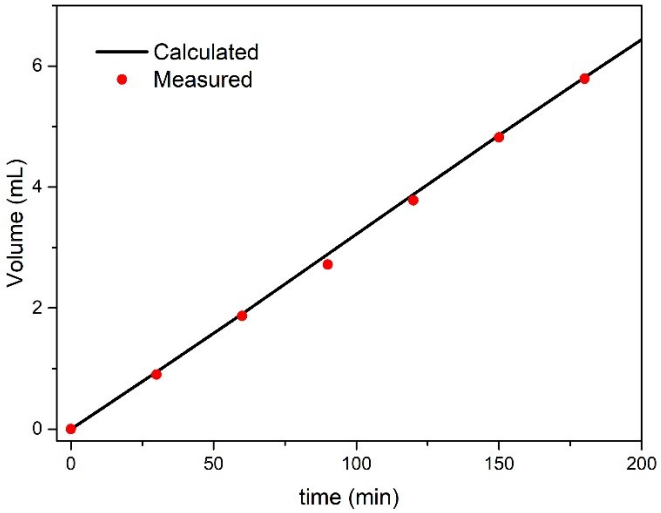

Figure S8. Electrocatalytic Faradaic efficiency of oxygen production over $FeCoNiF(OH)_x$ at the current density of 100 mA cm^{-2}.

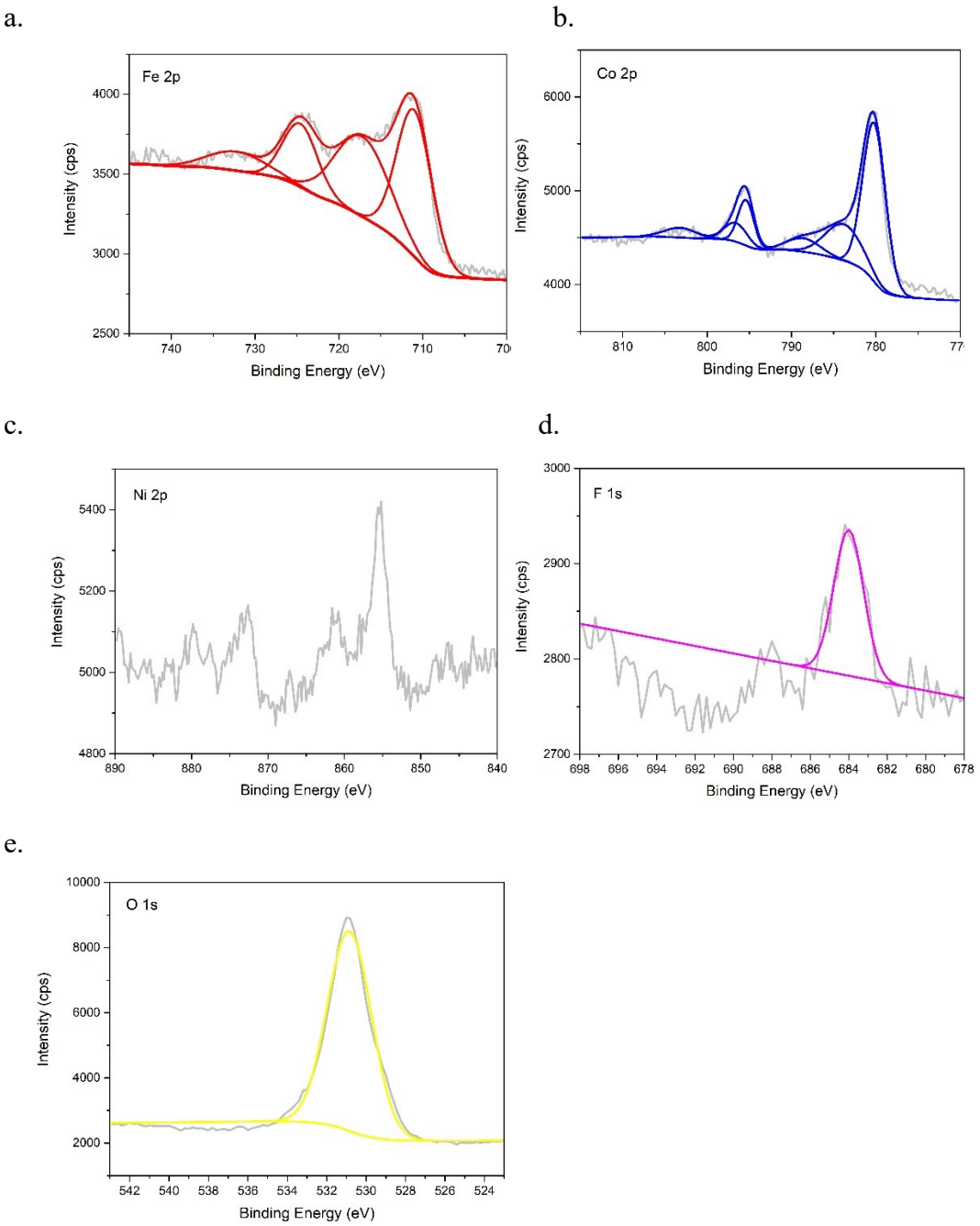

Figure S9. XPS spectra of $FeCoNiF(OH)_x$ after CPE.

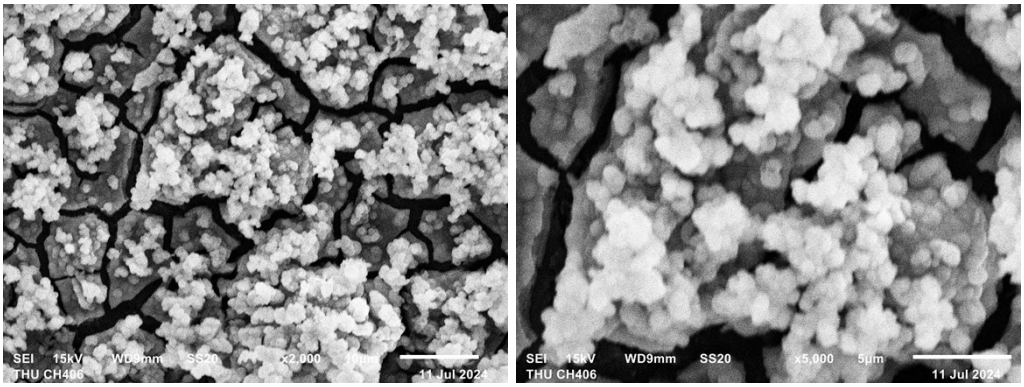

Figure S10. SEM images of $FeCoNiF(OH)_x$ after CPE.

a. b.

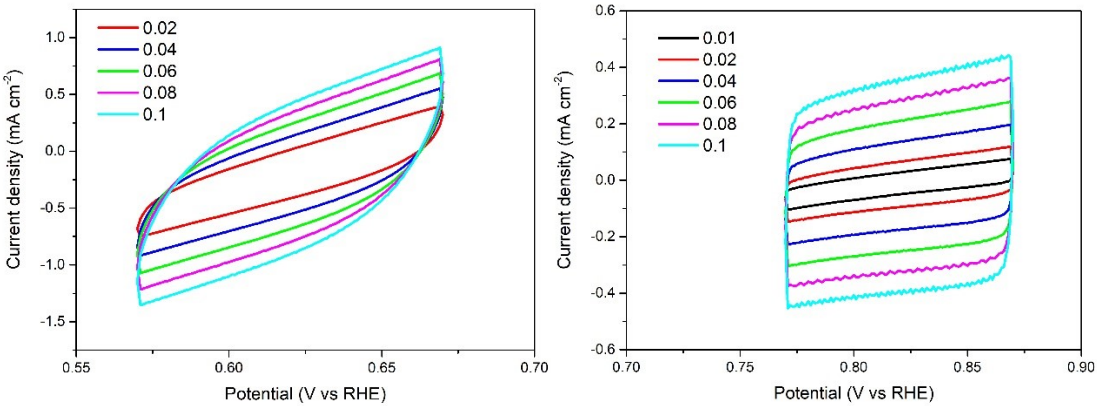

Figure S11. CV curves of (a) $FeCoNiF(OH)_x$ and (b) $FeCoNi(OH)_x$ in 1.0 M KOH at different scan rates of 10, 20, 40, 60, 80 and 100 mV s^{-1}.

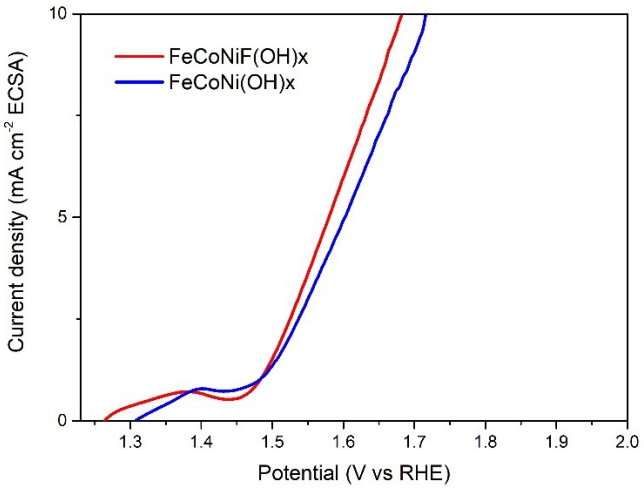

Figure S12. LSV curves from Fig. 3a normalized to the electrochemical active surface area (ECSA).

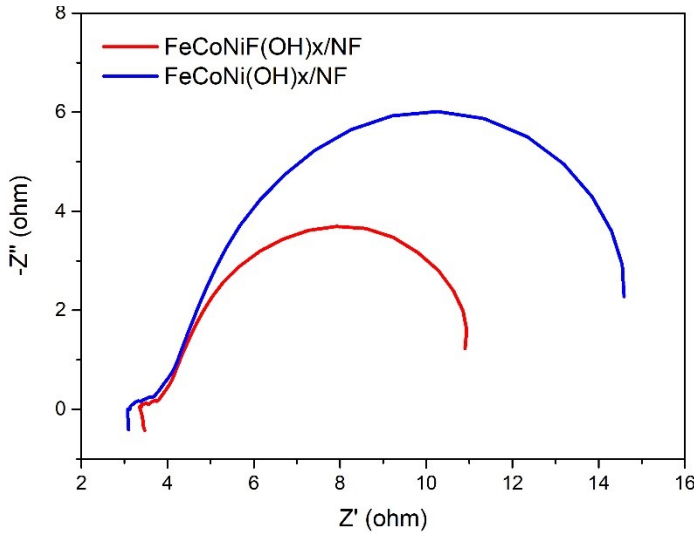

Figure S13. Nyquist plots of electrochemical impedance spectra of $FeCoNiF(OH)_x$ and $FeCoNi(OH)_x$ at η = 243 mV.

Table S1. Element distributions of $FeCoNiF(OH)_x$ and $FeCoNi(OH)_x$.

	ICP-MS		
	Fe (%)	Co (%)	Ni (%)
$FeCoNiF(OH)_x$	38.7±2.6	44.6±2.5	16.7±0.8
$FeCoNiF(OH)_x$ sample 1	38.1	46.0	15.9
$FeCoNiF(OH)_x$ sample 2	41.5	41.5	17.0
$FeCoNiF(OH)_x$ sample 3	38.0	45.9	16.1
$FeCoNiF(OH)_x$ sample 4	41.4	41.8	16.9
$FeCoNiF(OH)_x$ sample 5	34.6	47.6	17.8
$FeCoNi(OH)_x$	43.5±3.9	39.2±2.1	17.3±1.9
$FeCoNi(OH)_x$ sample 1	47.3	37.7	15.0
$FeCoNi(OH)_x$ sample 2	47.5	37.2	15.3
$FeCoNi(OH)_x$ sample 3	43.0	39.0	18.0
$FeCoNi(OH)_x$ sample 4	42.8	39.0	18.2
$FeCoNi(OH)_x$ sample 5	36.9	43.1	20.0